

Monodromy and Poncelet Families

Richard Evan Schwartz *

August 9, 2008

1 The Main Results

Let P be a twisted n -gon with corner invariants \dots, x_1, x_2, \dots . This sequence has period $2n$. Let Ω_1 be the monodromy matrix associated to P and let Ω_2 be the dual monodromy matrix. We have the formulas

$$\Omega_1 = \frac{(\sum_{k=0}^{\lfloor n/2 \rfloor} O_k)^3}{O_n^2 E_n}; \quad \Omega_2 = \frac{(\sum_{k=0}^{\lfloor n/2 \rfloor} E_k)^3}{E_n^2 O_n}. \quad (1)$$

Here $\lfloor n/2 \rfloor$ is the floor of $n/2$. For convenience, we always take n even so that $\lfloor n/2 \rfloor = n/2$. The polynomials $O_1, E_1, O_2, E_2, \dots$ are the *monodromy invariants*. The terms of O_k and E_k are homogeneous polynomials respectively of weight $-k$ and k relative to a scaling operation. See Equation 2 below.

We wish to consider these invariants for (closed) Poncelet polygons. We will consider two poncelet polygons P and P' from the same family. This means that P and P' are both inscribed in a conic C_1 and superscribed about another conic C_2 . We usually take C_1 to be the unit circle (or its complexification). We only consider the generic case, when C_1 and C_2 are in general position. In this case, we call P and P' related. Our purpose is to prove the following result.

Theorem 1.1 *If P and P' are related Poncelet n -gons then $O_k(P) = O_k(P')$ and $E_k(P) = E_k(P')$ for $k = 1, \dots, (n/2), n$.*

* Supported by N.S.F. Research Grant DMS-0072607

The result also holds in the odd case, and the proof is similar. We treat the even case just for convenience. We will deduce Theorem 1.1 from two lemmas. The first lemma is a special case of Theorem 1.1.

Lemma 1.2 $E_n(P') = E_n(P)$ and $O_n(P) = O_n(P)$.

The second lemma involves the scaling operation we mentioned above. For $t \in \mathbf{R}$, let P_t denote the twisted n -gon with invariants

$$\dots tx_0, t^{-1}x_1, tx_2, t^{-1}x_3, \dots,$$

normalized so that $V_t(j) = V(j)$ for $j = 1, 2, 3, 4$. Here $V(j)$ is the j th vertex of P and $V_t(j)$ is the j th vertex of P_t .

Lemma 1.3 *There are infinite many values t for which $\Omega_1(P_t) = \Omega_1(P)$ and $\Omega_2(P_t) = \Omega_2(P)$.*

Proof of Theorem 1.1: Let t be any of the values from Lemma 1.3. We have the general homogeneity relations:

$$E_k(P_t) = t^k E_k(P); \quad O_k(P_t) = t^{-k} O_k(P). \quad (2)$$

Lemma 1.2 combines with Equation 2 to give

$$E_n(P_t) = E_n(P); \quad O_n(P_t) = O_n(P). \quad (3)$$

Combining Equations 1, Equation 2, Equation 3, and Lemma 1.3, we have

$$\sum_{k=1}^{n/2} t^k (E_k(P) - E_k(P')) = 0, \quad (4)$$

for all t near 1. But then we have a polynomial with infinitely many roots. Hence, all the coefficients are 0. That is, $E_k(P) = E_k(P')$ for all k . Similarly $O_k(P) = O_k(P')$ for all k . ♠

We will prove Lemmas 1.2 and 1.3 by the same technique, which we now describe. The idea is to complexify. Over \mathbf{C} , the set of Poncelet polygons related to P is parametrized by a complex torus \mathbf{T} . One identifies the points on \mathbf{T} with *flags* (p, L) , where $p \in C_1$ and L is a line through p and tangent to C_2 . There are two kinds of Poncelet polygons in this family, *ordinary* and

degenerate. The ordinary Poncelet polygons are those consisting of n distinct points in general position. The rest of the polygons we call *degenerate*. (Below we will analyze the structure in detail.) We classify the points of \mathbf{T} as *ordinary* and *degenerate*, according to the type of polygon they correspond to. There are finitely many degenerate points.

Let $f : \mathbf{T} \rightarrow \mathbf{C}$ denote the function $f(z) = E_n(P^z)$. Here P^z is the Poncelet polygon whose 1st and 2nd vertices determine the flag associated to z . The vertex of the flag is $V^z(1)$ and the line contains $V^z(1)$ and $V^z(2)$. The function f is a *rational function* on \mathbf{T} . By this we mean that f is holomorphic away from the degenerate points of T , and f has a Laurent series in the neighborhood of each degenerate point. That is, f has no essential singularities. We will prove the following result.

Lemma 1.4 *For each degenerate point $z \in \mathbf{T}$ there is a sequence $\{z_j\}$ of ordinary points such that $z_j \rightarrow z$ and $\{f(z_j)\}$ is bounded.*

Since f is a rational function, Lemma 1.4 implies that f has no poles on \mathbf{T} . Hence f is constant. This proves Lemma 1.2.

We will take a similar approach to Lemma 1.3. There is an action of D_n , the order $2n$ dihedral group, on \mathbf{T} , such that the orbits are exactly the flags corresponding to Poncelet polygons. We describe this action below in detail. We call two points of \mathbf{T} *equivalent* if they are in the same D_n orbit.

Lemma 1.5 *For each degenerate point z' there is an equivalent degenerate point z with the following property. If t is sufficiently close to 1 then there is a sequence $\{z_j\}$, converging to z , such that*

- $P_t^{z_j}$ exists.
- $\lim_{j \rightarrow \infty} P_t^{z_j}$ is a well-defined twisted n -gon.

Let $g_t(z) = \Omega_1(P_t^z)$ and $h_t(z) = \Omega_2(p_t^z)$. Lemma 1.5 covers one degenerate point per equivalence class. Lemma 1.5 says that the functions g_t and h_t have no poles at our special points. But the unordered pair $\{g_t, h_t\}$ is constant on D_n -orbits. Hence, g_t and h_t have no poles at all. Hence, these functions are constant. This proves Lemma 1.3.

The rest of the paper is devoted to proving Lemmas 1.4 and 1.5.

2 The Complex Picture

The complex torus \mathbf{T} arises in the proof of the Poncelet porism. For $j = 1, 2$ we have maps $\phi_j : \mathbf{T} \rightarrow C_j$ given by

$$\phi_1(z) = p; \quad \phi_2(z) = L \cap C_2; \quad z = (p, L). \quad (5)$$

Both ϕ_1 and ϕ_2 are double branched-covers. The map ϕ_1 is branched over the 4 points of $C_1 \cap C_2$. The map ϕ_2 is branched over the points of $x \in C_2$ such that the line tangent to C_2 at x is also tangent to C_1 . There are 4 such points.

There is some real plane $X \subset \mathbf{CP}^2$ such that $C_1 \cap C_2 \subset X$, and also all common tangent lines lie in X . We can identify X with \mathbf{R}^2 . The picture then looks like Figure 1.

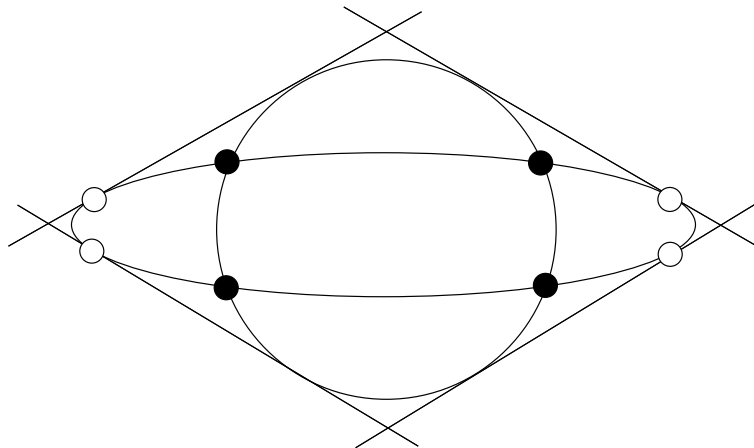


Figure 1: all the branch points

The *singular points* of ϕ_j are the pre-images of the branch points. There are 4 such points. When uniformized, \mathbf{T} is obtained by gluing the opposite sides of a rectangle in the obvious way. Referring to Figure 2, the black points indicate the singular points of ϕ_1 and the white points indicate the singular points of ϕ_2 . Reflection in the vertical centerline swaps black and white points. The dotted horizontal lines are $\phi_1^{-1}(C_1)$. This well-known structure is recalled in my paper on the Poncelet Grid. ¹

¹Our picture here differs from the one there only in that we are rotating the torus by 90 degrees so as to switch the roles played by horizontal and vertical.

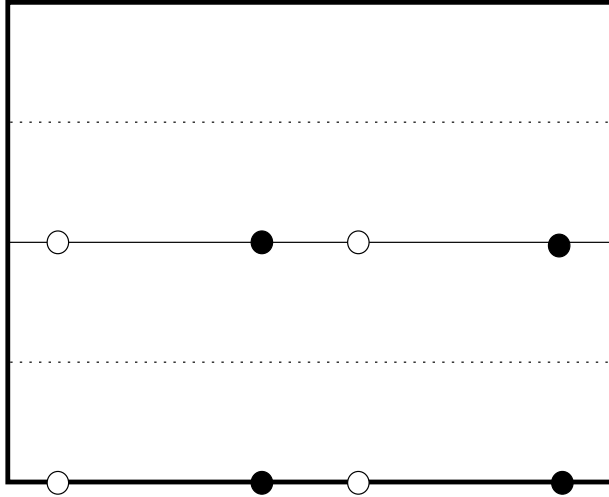


Figure 2: singular points

There is an involution $I_j : \mathbf{T} \rightarrow \mathbf{T}$ that commutes with ϕ_j . The involution I_j fixes the singular points of ϕ_j . The group $D_n = \langle I_1, I_2 \rangle$ is the dihedral group of order $2n$. The map ϕ_1 maps the D_n -orbits to Poncelet polygons. The Poncelet polygon is ordinary iff its image has n points. This happens iff the orbit does not contain one of the singular points of ϕ_1 or ϕ_2 . Thus, there are $4n$ degenerate points. Each degenerate point is equivalent under D_n to one of the singular points. $2n$ of these degenerate points lie on the center horizontal line in Figure 2, hereafter called *the centerline* and denoted by Ξ . The other $2n$ lie on the bottom/top horizontal edge of the rectangle. By symmetry, it suffices to consider the ones on the centerline.

Figure 3 shows the degenerate points arranged along Ξ in case $n = 4$. The endpoints of Ξ are identified, so that Ξ is really a circle. The degenerate points on the Ξ are arranged into two D_n -orbits. One of the orbits consists of the black points and the other orbit consists of the white points. This picture is representative of the even cases n . Referring to Lemma 1.5 we just need to analyze these two special orbits.

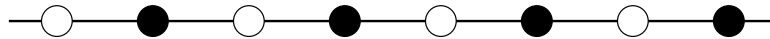


Figure 3: degenerate points on the centerline

For the odd cases, the picture is a bit different, and for convenience we ignore it.

3 Models for the Degenerations

We already mentioned that we only consider the case when n is even. As another convenience, we take n large, say $n > 100$. The purpose of taking n large is so that we can isolate the (two) parts of a degenerate Poncelet polygon that cause us trouble.

Let Ξ denote the centerline of \mathbf{T} . The map $\phi_1 : \Xi \rightarrow C_1$ is a 2-to-1 folding map. The two singular points on Ξ are mapped to the two upper intersection points of $C_1 \cap C_2$, and $\phi_1(\Xi)$ is precisely the uppermost arc of $C_1 - C_2$. Outside any neighborhood U of the two singularities of ϕ_1 , the map ϕ_1 is C_U -bilipschitz. Here C_U depends on the neighborhood U . Here Ξ is given its uniformized metric and C_1 is given its usual metric.

We call the singular orbits on Ξ by O_1 and O_2 . These orbits have the following description.

1. O_1 is the D_n -orbit of the 2-singularities of ϕ_1 that lie on Ξ – the black points in Figure 3. The restriction of ϕ_1 to O_1 is 2-to-1 on all but 2 points of this orbit. the image $\phi_1(O_1)$ consists of $(n/2) + 1$ points.
2. O_2 is the D_n -orbit of the 2-singularities of ϕ_2 that lie on Ξ – the white points in Figure 3. In this case, $\phi_1(O_1)$ maps this orbit to C_1 in a 2-to-1 fashion.

Given the folding nature of ϕ_1 , Figure 4 shows a fairly accurate picture of one end of $\phi_1(O_1)$ and $\phi_1(O_2)$. The other end is the mirror reflection. The points in the middle are not really of interest to us. In the first case, the point labelled 5 is the branch point.

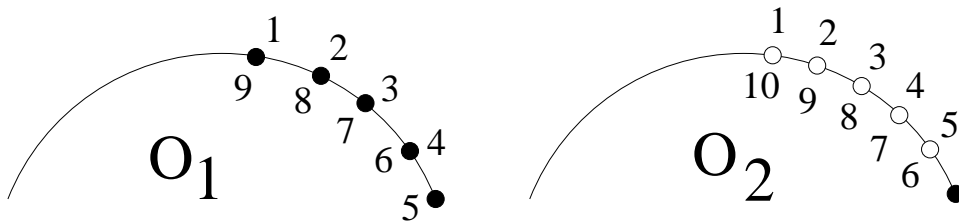


Figure 4: local picture of the degenerate polygons

For small ϵ , the D_n -orbit O_j^ϵ that is ϵ away from O_j is obtained from O_j by replacing each point of O_j by two points, on either side, that are 2ϵ apart. The picture of $\phi_1(O_1^\epsilon)$ corresponding to Figure 4 is obtained by replacing the

points commonly labelled $(1, 9)$ $(2, 8)$, $(3, 7)$ and $(4, 6)$ each by two points that are between $C^{-1}\epsilon$ and $C\epsilon$ apart. Here C is a positive constant that only depends on n . For O_2 the picture is similar, except that all points are split apart. The estimate on the spacing comes from the bi-lipschitz nature of ϕ_1 away from the singularities.

We find it convenient to apply a projective transformation that moves C_1 to the standard parabola

$$\Pi = \{(x, y) \mid y = x^2\} \tag{6}$$

carries the rightmost points in our pictures to $(0, 0)$. Such a projective transformation is bi-lipschitz. To draw pictures in Π , we consider the projection onto the first coordinate. Figure 6 shows a fairly accurate picture of one end of (the renormalized image of) $\phi_1(O_j^c)$.

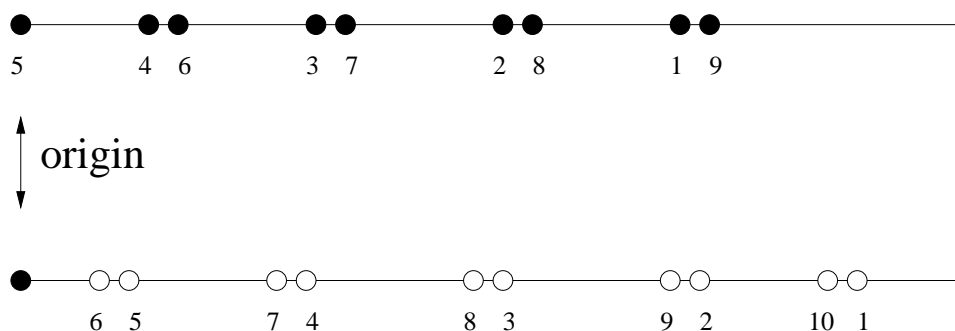


Figure 6: local model of the degenerations

The left endpoint is the origin. The only point we have not justified is the ordering of the points in Figure 6. The order we have drawn follows from the way D_n acts on Ξ . Alternatively, this order can be determined experimentally in one case; then the order remains unchanged in all cases by continuity. Again, we are showing the first coordinates of our points. They really lie on the parabola Π . Whether we consider the points on Π or just the first coordinates, the spacing between nearby points is between $C^{-1}\epsilon$ and $C\epsilon$, and the spacing between all other pairs of points is at least C^{-1} . Here C only depends on n .

Figure 6 gives us our local model for the way the Poncelet polygons degenerate at one end. The other end, halfway around in terms of the ordering on the points, is similar. The points in the middle play little role in the analysis, though sometimes we will have to consider these points in a very general sort of way.

4 Proof of Lemma 1.4

4.1 Reduction to Three Estimates

Let

$$\chi(a, b, c, d) = \frac{(a-b)(c-d)}{(a-c)(b-d)}. \quad (7)$$

Here χ is the inverse of the cross ratio. We define the corner invariants of interest to us by example.

$$\chi_1 = \chi(V(1), V(2), L(12) \cap L(34), L(12) \cap L(45)) \quad (8)$$

Here $L(ij)$ is the line through $V(i)$ and $V(j)$. The corner invariant χ_2 is obtained by shifting all indices by 1. And so on. Our function E_n is the product $\prod \chi_j$.

For ease of exposition, we will just consider the orbits O_1^ϵ . The orbits O_2^ϵ have an almost identical treatment. Referring to our model in Figure 6, we just have to show that $\chi_2\chi_3\chi_4$ remains bounded as $\epsilon \rightarrow 0$. For other nearby indices, the corner invariants involve 5 points that remain in general position even in the limit. The singularity at the other end has the same analysis.

4.2 The First Estimate

Figure 7 shows the situation for χ_2 . This invariant computes the inverse cross ratio $\chi(a, b, c, d)$. From our model, we get

$$\|c - d\| = O(\epsilon); \quad \|x - y\| = O(1); \quad x \in \{a, b\} \quad y \in \{c, d\}. \quad (9)$$

Hence $\chi_2 = O(\epsilon)$. Our notation $f = O(g)$ means that f/g lies between two positive constants that depend only on n .

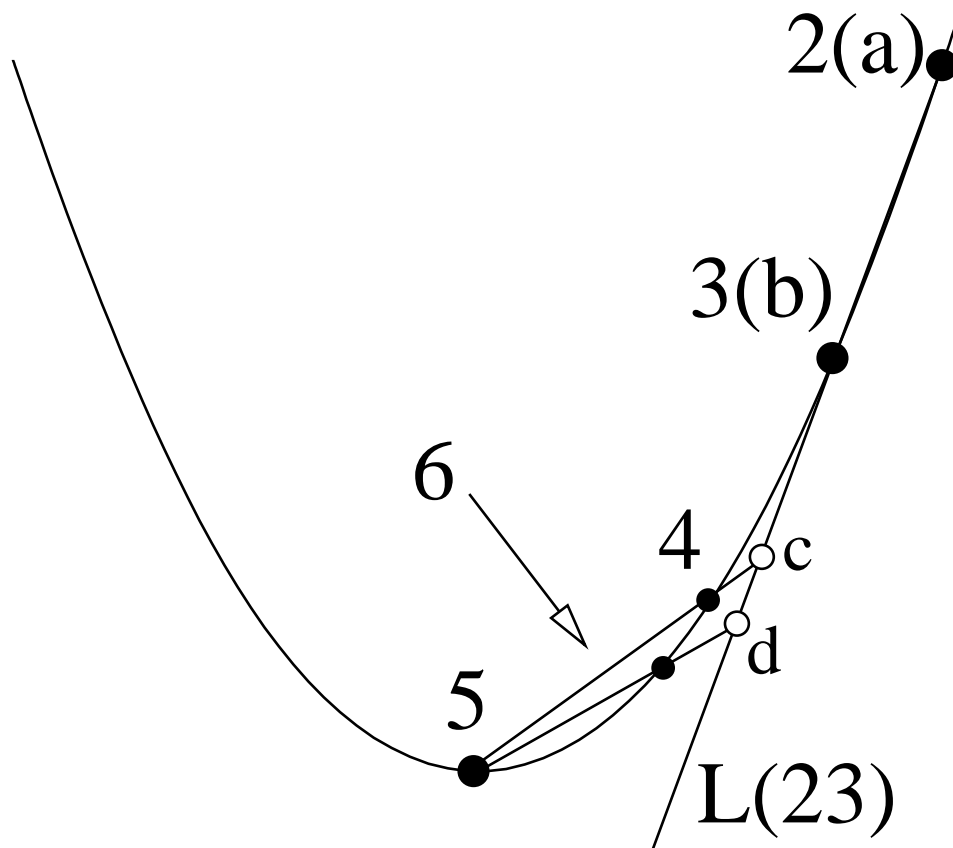


Figure 7: Estimating χ_2 .

4.3 The Second Estimate

Figure 8 shows the situation for χ_3 . The points of interest to us are

$$a = V(3); \quad b = V(4); \quad c = L(56) \cap L(34); \quad d = L(67) \cap L(34).$$

The (inverse) cross ratio is taken in the order we have listed the points. There is an $O(1)$ -bilipschitz projective map that carries $V(3), V(7), V(4), V(6)$ to the vertices of a rectangle. (We mean that the transformation is $O(1)$ -bilipschitz on the convex hull of these points.) From this, we conclude that

$$\|d - b\| = O(1); \quad \|d - a\| = O(1).$$

But then $\|d - c\| = O(1)$ as well. Also, $\|a - b\| = O(1)$ and $\|a - c\| = O(1)$. Hence $\chi_3 = O(1)$.

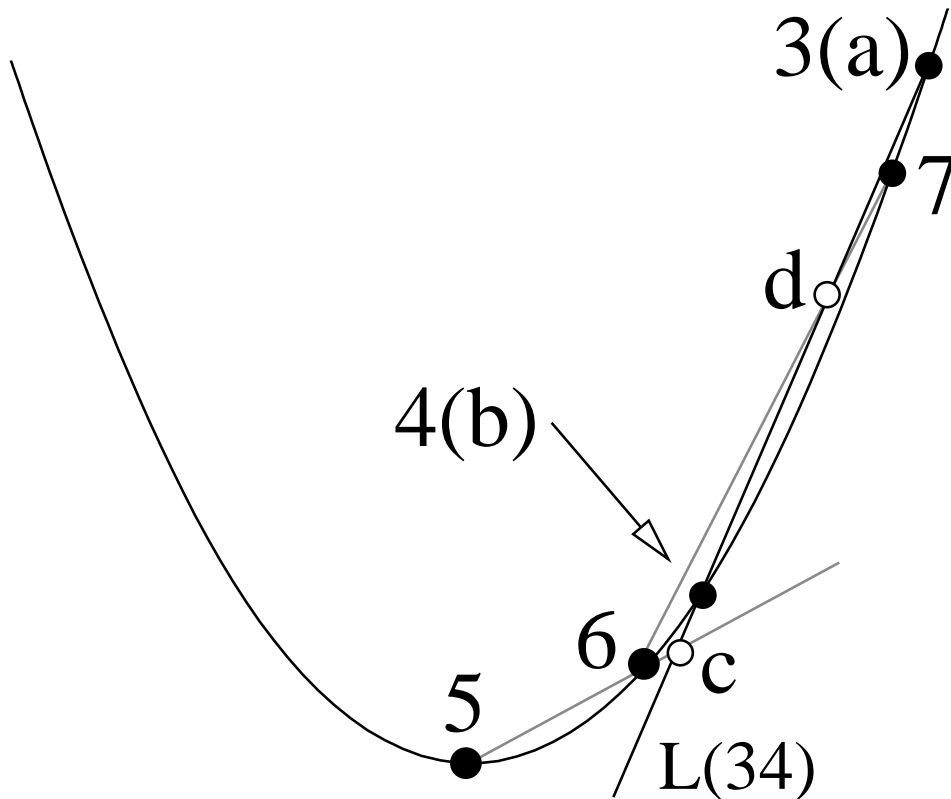


Figure 8: Estimating χ_3 .

More is true in this case, since $\|b - c\| = O(\epsilon)$ we conclude that

$$\left| 1 - \frac{\|a - b\|}{\|a - c\|} \right| = O(\epsilon); \quad \left| 1 - \frac{\|d - b\|}{\|d - c\|} \right| = O(\epsilon).$$

From this, we see that

$$\left| 1 - \chi_3(P^\epsilon) \right| = O(\epsilon). \tag{10}$$

4.4 The Third Estimate

Figure 9 shows the situation for χ_4 . The points of interest to us, in order, are

$$a = V(4); \quad b = V(5); \quad c = L(67) \cap L(45); \quad d = L(68) \cap L(45).$$

In the same sense as the previous case, there is a uniformly bilipschitz projective map that carries $V(5), V(6), V(4), V(7)$ to a trapezoid whose 3 long sides have length 1 and whose short side has length ϵ . From this, we get

$$\|c - a\| = O(\epsilon). \quad (11)$$

Consider the triangle $(V(4), V(7), d)$. The small angles of this triangle are all $O(1)$. Also, one side of this triangle, namely the one connecting $V(4)$ to $V(7)$, has length $O(1)$. Hence all sides have length $O(1)$. In particular,

$$\|d - a\| = O(1) \quad (12)$$

But then we have $\|c - d\| = O(1)$ and $\|b - d\| = O(1)$. Finally, $\|b - a\| = O(1)$. Hence $\chi_4 = O(\epsilon^{-1})$.

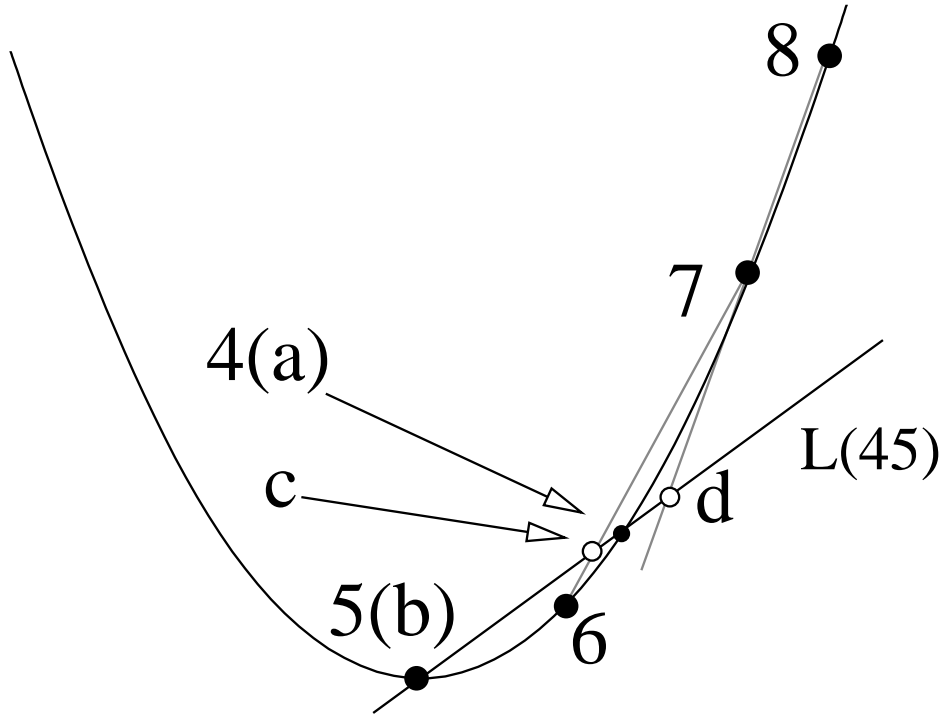


Figure 9: Estimating χ_4 .

Putting everything together, and slightly abusing the notation, we have

$$\chi_2 \chi_3 \chi_4 = O(\epsilon) O(1) O(\epsilon^{-1}) = O(1).$$

This completes the proof of Lemma 1.2.

5 Variation of Pentagons

As preparation for proving Lemma 1.5, we establish a fact about the corner invariants. Given a pentagon with vertices $V(1), \dots, V(5)$, we define

$$\chi_1^+ = \chi(V(1), V(2), L(12) \cap L(34), L(12) \cap L(45)) \quad (13)$$

$$\chi_5^- = \chi(V(5), V(4), L(54) \cap L(32), L(54) \cap L(21)) \quad (14)$$

We now consider a family $\{P_t\}$ of pentagons with t a parameter near 1.

Lemma 5.1 *Let P be a strictly convex pentagon and let $\{P_n\}$ be a sequence of strictly convex pentagons such that*

1. $V_n(k) \rightarrow V(k)$ for $k = 1, 2, 3, 4$.
2. $\chi_1^+(P_n) \rightarrow \chi_1^+(P)$
3. $\chi_5^-(P_n) \rightarrow \chi_5^-(P)$

Then $V_n(5) \rightarrow V(5)$

Proof: We normalize so that the vertices $V(1), V(2), V(4), V(5)$ are the vertices of a unit square, as in Figure 10. Let T_n be a projective transformation such that $T_n(V_n(k)) = V(k)$ for $k = 1, 2, 4, 5$. Referring to Figure 10, we have

$$a = \chi_1^+; \quad b = \chi_5^-$$

But a and b determine the location of $V(3)$. From these facts, and from our hypotheses, we see that $T_n(V_n(3)) \rightarrow V(3)$.

Now we see that $V_n(k) \rightarrow V(k)$ for $k = 1, 2, 3, 4$ and $T_n(V_n(k)) \rightarrow V(k)$ for $k = 1, 2, 3, 4$. Since these points are all in general position, this forces $T_n \rightarrow I$, the identity transformation. Hence $P_n \rightarrow P$. ♠

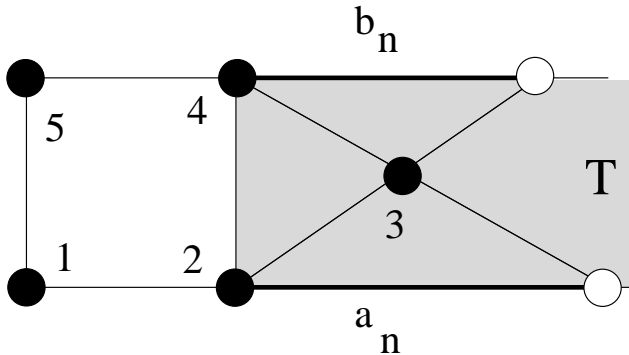


Figure 10: compactness argument

5.1 Lemma 1.5 Modulo a Detail

We fix some large value of n . As in the proof of Lemma 1.4, we will just deal with the degenerations associated to the orbit O_1 . The proof for the degenerations associated to O_2 is essentially the same.

Let P^ϵ denote the Poncelet polygon associated to the perturbed orbit O_1^ϵ . In constructing P_t^ϵ we normalize so that the vertices labelled 2, 3, 4, 5 are independent of t . Let P denote the degenerate Poncelet polygon corresponding to $\epsilon = 0$. We use our model from Figure 6. The purpose of this section is to prove the following result

Lemma 5.2 (Variation) *Suppose that $\{(\epsilon_n, t_n)\}$ is any sequence converging to $(0, 1)$. Then*

$$V_{t_n}^{\epsilon_n}(k) \rightarrow V(k); \quad k = 6, 7, 8$$

We prove this result in the next section. In the following lemma, we take the indices mod n on the right hand side of the main equation.

Corollary 5.3 *Suppose that $\{(\epsilon_n, t_n)\}$ is any sequence converging to $(0, 1)$. Then*

$$V_{t_n}^{\epsilon_n}(k) \rightarrow V([k]); \quad k \geq 6.$$

Proof: Let $\chi_k^+ = \chi_k$, the invariants we considered in the proof of Lemma 1.4. We let χ_{-k}^- denote the invariant obtained by negating all the indices used in the definition of χ_k^+ . Then χ_k^+ and χ_k^- . To summarize our proof of Lemma 1.4, we showed

$$\chi_2^+(P_1^\epsilon) = O(\epsilon); \quad \chi_4^+(P_1^\epsilon) = O(\epsilon^{-1}) \quad (15)$$

and $\chi_k^+(P_1^\epsilon) = O(1)$ for all nearby k . The same argument shows that

$$\chi_6^-(P_1^\epsilon) = O(\epsilon^{-1}); \quad \chi_8^-(P_1^\epsilon) = O(\epsilon) \quad (16)$$

and $\chi_k^- = O(1)$ for all nearby k . For convenience, we repeat the relevant half of Figure 6.

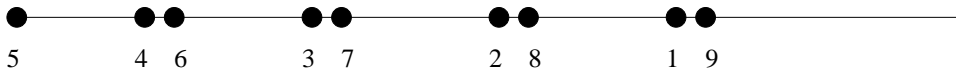


Figure 11: local model of the degeneration

For convenience, we use the notation

$$V_n(k) = V_{t_n}^\epsilon(k).$$

We focus our attention on the pentagon

$$V_n(5), \dots, V_n(9) \tag{17}$$

From the Variation Lemma and our normalization, which takes care of $V_n(5)$, we see that $V_n(k) \rightarrow V(k)$ for $k = 5, 6, 7, 8$. The pentagon made from $V(k)$ for $k = 5, 6, 7, 8, 9$ is strictly convex, and both $\chi_5^+(P^\epsilon)$ and $\chi_9^-(P^\epsilon)$ exist, are finite, and are continuous at $\epsilon = 0$. Hence

$$\chi_5^+(P_n) \rightarrow \chi_5^+(P); \quad \chi_9^-(P_n) \rightarrow \chi_9^-(P).$$

By Lemma 5.1, we now see that the conclusion of the Variation Lemma holds for $k = 9$.

Now we can repeat this argument, shifting the indices by 1. hence, the conclusion of the Variation Lemma holds for $k = 10$. Continuing in this way, we see that Variation Lemma holds for all $k = 5, \dots, (n/2) + 5$.

We have made our analysis under the assumption that the vertices $V_n(k)$ are fixed, for $k = 2, 3, 4, 5$. However, we would get the same conclusion if these vertices varied in a way such that $V_n(k) \rightarrow V(k)$ for $k = 2, 3, 4, 5$. We could adjust the picture, for each n , by a projective transformation T_n that converges to the identity.

We have established that

$$V_n(k + n/2) \rightarrow V(k + n/2); \quad k = 2, 3, 4, 5$$

Our analysis in the proof of Lemma 1.4 works equally well for the degeneracy corresponding to the index $(n/2) + 5$. We conclude that the Variation Lemma holds when we shift indices by $n/2$. But then we can repeat our argument above. We conclude that the Variation Lemma holds for $k = (n/2) + 6, \dots, n + 5$. Now we can repeat the argument and take care of the next $n/2$ vertices, and so on. ♠

Proof of Lemma 1.5: If Lemma 1.5 is false, then for every $\epsilon > 0$, we can find some t , arbitrarily close to 1, such that P_t^ϵ does not converge to P on the first n vertices. But this contradicts the result we just established. This proves Lemma 1.5 modulo the Variation Lemma. ♠

6 Some Auxilliary Cross Ratios

We need to understand the geometry of some of other cross ratios before making out estimate. Let s_{ij} denote the slope of the line containing $V(i)$ and $V(j)$. Let

$$\widehat{\chi}_5 = \chi(s_{35}, s_{45}, s_{65}, s_{75}). \quad (18)$$

Normalizing as in Lemma 5.1, we compute easily that

$$\widehat{\chi}_5 = \chi_3^+ \chi_7^-. \quad (19)$$

Therefore

$$\widehat{\chi}(P_t^\epsilon) = \widehat{\chi}(P^\epsilon). \quad (20)$$

This particular invariant does not change under the rescaling. Equation 10 says that $\chi_3^+(P^\epsilon) \rightarrow 1$ as $\epsilon \rightarrow 0$. The symmetric argument gives the same result for $\chi_7^-(P^\epsilon)$. Hence $\widehat{\chi}_5(P^\epsilon) \rightarrow 1$ as $\epsilon \rightarrow 0$.

Lemma 6.1 $\widehat{\chi}_5(P^\epsilon) < C\epsilon^2$ for some constant C that only depends on n .

Proof: Let \mathbf{T} denote the complex torus of flags, constructed above. Let $\tau(z)$ denote the function that computes the first corner invariant of P^z , the Poncelet polygon corresponding to z . We put local coordinates on the centerline so that it is the x -axis, and the black singular point corresponds to 0. From the way we have set things up, we have

$$\chi_3^+(P^\epsilon) = \tau(\epsilon); \quad \chi_7^-(P^\epsilon) = \tau(-\epsilon).$$

Therefore

$$\widehat{\chi}_5(P^\epsilon) = \tau(\epsilon)\tau(1 - \epsilon).$$

Equation 10 says that we can write the Taylor series expansion

$$\tau(z) = 1 + C_1 z + C_2 z^2 + \dots$$

Therefore

$$\tau(\epsilon) = 1 + C_1 \epsilon + C_2 \epsilon^2 \dots; \quad \tau(-\epsilon) = 1 - C_1 \epsilon + C_2 \epsilon^2 \dots$$

Multiplying these two expressions, the coefficient of ϵ cancels, and we get

$$\tau(\epsilon)\tau(-\epsilon) = 1 + C_2' \epsilon^2 + C_3' \epsilon^3 \dots$$

This proves what we want. ♠

7 Proof of the Variation Lemma

7.1 The First Estimate

We treat the case $k = 6$ of the Variation Lemma. First of all, we have

$$\widehat{\chi}_4(P_n) = \widehat{\chi}_4(P_{t_n}^{z_n}) = \widehat{\chi}_4(P^{z_n}). \quad (21)$$

The first equality is just a definition. The second one says that the given cross ratio is independent of t .

It follows from Equation 21 that

$$L_n(4, 6) \rightarrow L(46). \quad (22)$$

Here $L(46)$ is the tangent line to the parabola Π at $V(4) = V(6)$. Referring to Figure 12, the points c_n and d_n depend on n . But $\chi_2^+(P_n) = t_n \epsilon_n \rightarrow \epsilon_n$. But this forces

$$\frac{\|V_n(6) - V(6)\|}{\|V(6) - V(4)\|} \rightarrow 0 \quad \|V_n(6) - V(4)\| = O(\epsilon_n). \quad (23)$$

The first equation implies the second. The second restates the Variation Lemma for $k = 6$.

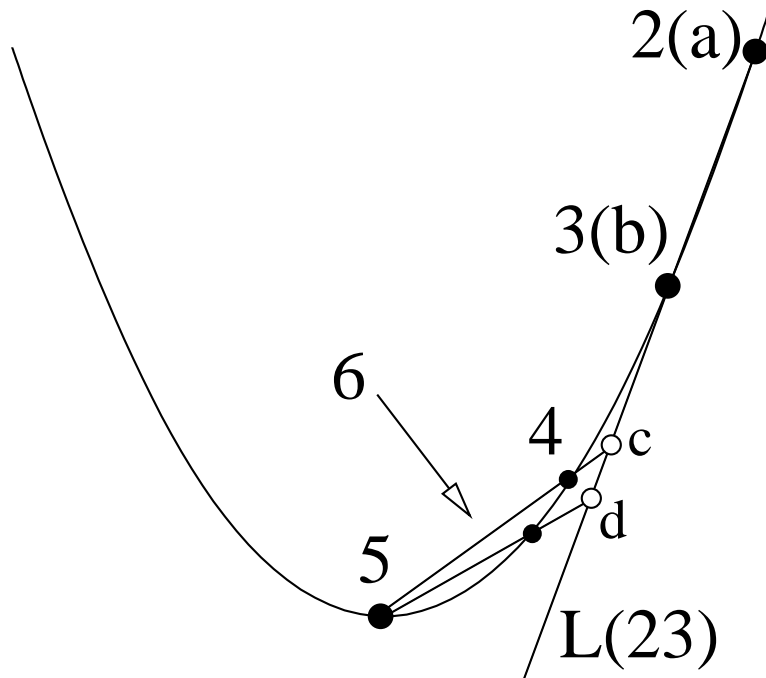


Figure 12: Estimating χ_2 .

7.2 The Second Estimate

Now we consider the case $k = 7$ of the Variation Lemma. We will establish two results.

1. As $n \rightarrow \infty$, the line $L_n(67)$ converge to the line $L(67)$.
2. As $n \rightarrow \infty$, the line $L_n(57)$ converge to the line $L(57)$.

Since the limiting lines have different slopes, and intersect only at $V(7)$, these two results combine to say that $V_n(7) \rightarrow V(7)$.

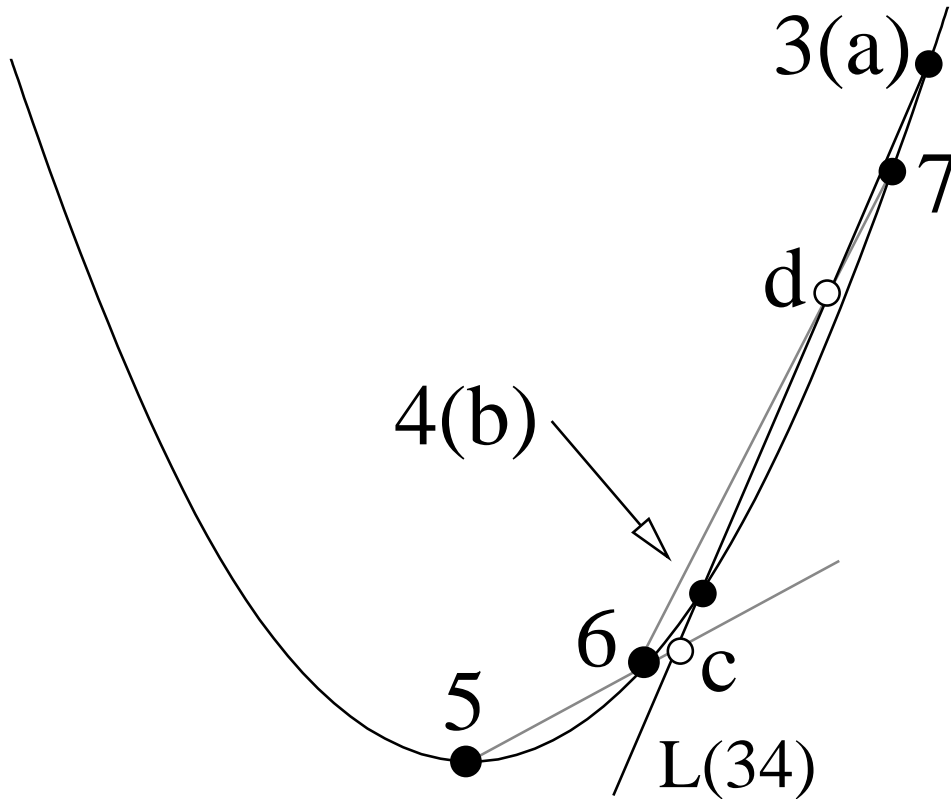


Figure 13: The relevant points

The first statement above uses Figure 8, which we repeat here as Figure 13. From our analysis of the case $k = 6$, we get

$$\|V_n(6) - V(4)\| = O(\epsilon_n); \quad L_n(64) \rightarrow L(64); \quad L_n(63) \rightarrow L(63). \quad (24)$$

Suppose that $L_n(67) \not\rightarrow L(67)$. Passing to a subsequence, we can assume

$$\text{angle}(L_n(67), L_n(63)) > C$$

But, referring to Figure 13, this big angle combines with Equation 24 to give

$$\|d - c\| = O(\epsilon_n)$$

But then $\chi_3^+(P_n)$ does not converge to 1. This contradicts Equation 10.

The second statement also uses Figure 13. We consider the cross ratio from the previous subsection. We have

$$\widehat{\chi}_5(P_n) = O(\epsilon_n^2). \quad (25)$$

It follows from our analysis in the case $k = 6$ that

$$\text{angle}(L_n(45), L_n(56)) = O(\epsilon_n). \quad (26)$$

The first of these lines is independent of n . Suppose that $L_n(57) \not\rightarrow L(57)$. Passing to a subsequence, we can assume

$$\text{angle}(L_n(57), L_n(53)) > C$$

But then

$$\widehat{\chi}_5(P_n) > C\epsilon_n,$$

contradicting Equation 25.

7.3 The Third Estimate

Now we consider the case $k = 8$ of the Variation Lemma. We will establish two results.

1. As $n \rightarrow \infty$, the line $L_n(68)$ converge to the line $L(68)$.
2. As $n \rightarrow \infty$, the line $L_n(78)$ converge to the line $L(78)$.

Since the limiting lines have different slopes, and intersect only at $V(8)$, these two results combine to say that $V_n(8) \rightarrow V(8)$.

Our arguments refer to Figure 9, which we reproduce here as Figure 14.

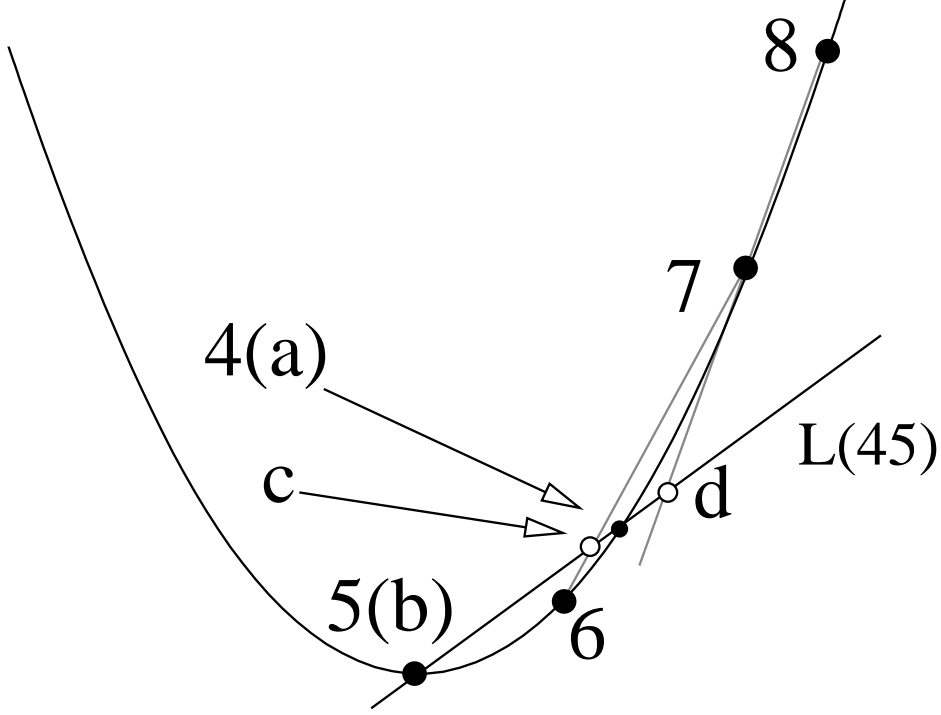


Figure 14: The relevant points

For the first statement, note that $\widehat{\chi}_6(P)$ exists because the lines $L(6k)$ are distinct for $k = 4, 5, 7, 8$. Moreover,

$$\widehat{\chi}_6(P_n) \Rightarrow \widehat{\chi}_6(P); \quad L_n(6k) \rightarrow L(6k); \quad k = 4, 5, 7. \quad (27)$$

This forces $L_n(68) \rightarrow L(68)$.

The last estimate is delicate. We consider the cross ratio $\chi_4^+(P_n)$, as shown in Figure 14. In Figure 14, the points a and b are independent of n and $c = c_n$ and $d = d_n$ depend on n . To show that $L_n(78) \rightarrow L(78)$ it suffices to show that $d_n \rightarrow d$. We introduce the auxilliary points

$$c'_n = c(P^{\epsilon_n}); \quad d'_n = d(P^{\epsilon_n}). \quad (28)$$

That is, we reconsider the picture when t_n is replaced by 1. Since $d'_n \rightarrow d$, it suffices to prove that

$$\left(\frac{\|d_n - b\|}{\|d_n - c\|} \right) / \left(\frac{\|d'_n - b\|}{\|d'_n - c\|} \right) \rightarrow 0. \quad (29)$$

Since $t_n \rightarrow 1$, we have

$$\frac{\chi_4^+(P^{\epsilon_n})}{\chi_4^+(P_n)} \rightarrow 1. \quad (30)$$

Recalling the definition of these invariants, and recalling that a and b are independent of n , we see that Equation 29 is equivalent to the statement that

$$\frac{\|c_n - a\|}{\|c'_n - a\|} \rightarrow 1. \quad (31)$$

This last equation follows from elementary geometry and three basic facts.

1. $L(45)$ and $L(67)$ are not parallel.
2. Letting $V'_n(7)$ denote Vertex 7 for P^{ϵ_n} , we have

$$\frac{\|V'_n(7) - V_n(7)\|}{\|V_n(7) - V_n(4)\|} \rightarrow 0.$$

- 3.

$$\frac{\|V'_n(6) - V_n(6)\|}{\|V_n(6) - V_n(4)\|} \rightarrow 0.$$

This completes our proof.